

# **A Mixed-Integer Nonlinear Programming Framework with Epidemiological and Vaccine Modeling for Patient Allocation During Pandemics**

**Alexander DeLise<sup>1</sup>, Seyedreza Abazari<sup>2</sup>, and Dr. Arda Vanli<sup>2</sup>**

<sup>1</sup>Department of Mathematics, <sup>2</sup>FAMU-FSU College of Engineering  
Florida State University  
Tallahassee, FL, USA  
ard221@fsu.edu, sabazari@fsu.edu, oavanli@eng.famu.fsu.edu

## **Abstract**

Pandemics strain healthcare systems worldwide, creating urgent challenges in allocating limited resources like hospital beds while controlling disease spread. Effective patient allocation during such crises is critical to minimizing unmet healthcare demand and ensuring equitable healthcare access across regions. This study addresses these issues by developing a mixed-integer nonlinear mathematical model that integrates Susceptible-Infected-Recovered-Vaccinated (SIRV) epidemic dynamics with patient transfer and allocation to improve patient distribution during outbreaks. Our approach also factors additional disease transmissions caused by the assignment of patients to different regions. Our model minimizes unmet demand per county for hospital beds and incorporates real-world data in the model parameters. We observe that in large metropolitan areas, where access to healthcare is critical, the vaccinated scenario exhibits significantly lower unmet hospital demand compared to the unvaccinated scenario, an outcome directly tied to the vaccines' success in lowering peak infection rates as demonstrated by the SIRV dynamics. The reduction in infection surges not only alleviates hospital capacity strain but also leads to fewer total patient transfers, underscoring the effectiveness of vaccination during pandemics. This research demonstrates the potential to enhance pandemic response strategies. The model provides policymakers and healthcare administrators with a robust, data-driven tool to make informed decisions, reducing strain on overburdened facilities and improving patient outcomes during pandemic scenarios.

**Keywords:** COVID-19, Patient Allocation, Data-Driven Optimization, Healthcare Systems, Epidemic Modeling

## **1. Introduction**

COVID-19 has presented significant obstacles for both detection and containment, particularly due to limited detection capabilities and varying incubation periods (Li et al. 2020; Lauer et al. 2020; Meyerowitz-Katz and Merone 2020). These challenges underscore the importance of refined epidemiological tracking and data-driven estimates of disease spread within populations when addressing issues that arise in pandemic scenarios. In general, compartmental epidemiological modeling and vaccination allocation strategies, especially when guided by precise data, can substantially moderate infection trajectories, even under moderate coverage (Waseel et al. 2024). Optimization-based methods have also demonstrated that strategic patient allocation can reduce overwhelming hospital demands, reflecting how operational and epidemiological approaches must align to mitigate pandemic impacts (Sarkar et al. 2021). These foundational insights on COVID-19 highlight the importance of robust modeling frameworks for patient allocation and the dynamic nature of disease spread.

Addressing pandemic surges in hospital demand requires systematic approaches to patient allocation that balance efficiency and equity in resource use. One stream of research leverages multi-objective linear programming to manage both ICU and non-ICU resources, demonstrating how coordinated decision-making can effectively limit hospital

overload (Aydin and Cetinkale 2022). Similarly, dynamic balancing methods based on forecasts of hospital bed occupancy have been shown to shift incoming patients among hospitals or regions, preventing local bottlenecks and ensuring smoother operations (Dijkstra et al. 2023). Robust multi-objective frameworks further integrate daily patient assignments with longer-term location planning into a single model, minimizing patient rejections, travel distances, and facility installation costs (Eriskin et al. 2024). Studies also highlight that tightly coupling patient routing with broader healthcare operations can significantly enhance service efficiency (Yinusa and Faezipour 2023; Shi 2023). By considering factors such as distance, inter-facility cooperation, bed capacity, and infection levels, these approaches emphasize the complexity of allocation decisions and the importance of dynamic, data-informed strategies for managing new COVID-19 cases during pandemics (Sarkar et al. 2021).

Compartmental disease models in literature capture intricate features of COVID-19 dynamics, such as partial immunity, quarantine policies, and heterogeneous transmission environments. Li et al. (2020) and Crokidakis (2020) have demonstrated that under-detection of confirmed cases can skew estimates of infection prevalence, prompting modifications to standard Susceptible-Exposed-Infected-Recovered (SEIR) frameworks. Others incorporate fractional-order mathematics or time-varying encounter networks to reflect the nuanced spread occurring in real-world transit systems (Kozioł et al. 2020; Mo et al. 2021). In some cases, interventions such as city-wide quarantine have been simulated in SEIR models to quantify the impact of lock down measures (Hou et al. 2020; He et al. 2020). Meanwhile, data-driven spatial risk classification and progressive vaccination plans have connected epidemiological models to tangible operational decisions, showing how high-risk locations can serve as entry points for disease control measures (Hong et al. 2024; Bennouna et al. 2023). Broader surveys also highlight the relationship between epidemic outbreaks and supply chain disruptions, emphasizing the critical need to effectively allocate patients to hospitals under high demand for scarce pandemic resources like vaccines (Queiroz et al. 2022; Anastassopoulou et al. 2020).

The COVID-19 pandemic has underscored the critical need for effective patient allocation strategies and, in many cases, inter-regional transfers to balance healthcare demand and capacity. From a macroscopic perspective, Della Rossa et al. (2020) propose a network model to simulate how the disease spreads across Italian regions, incorporating regional variations, long-distance travel, and ferry routes. Their findings suggest that targeted regional measures can help contain outbreaks and alleviate national-level pressures. In terms of operational optimization, linear and robust optimization models can be used to redistribute patient demand and resources, achieving at least a significant reduction in required surge capacity (Parker et al. 2020). Others, like in Hu et al. (2020), adopt queuing theory to adjust hospital bed allocations and control infections, demonstrating how prioritization ensures timely treatment for critically ill patients. Dynamic programming for bed allocation and patient subsidization highlight the benefits of subsidy schemes in reducing costs and wait times during medium pandemic surges (Ma et al. 2022). A broad overview of COVID-19 hospital surge capacity models stresses how these tools can predict and avert capacity constraints (Klein et al. 2022). Identifying excess hospital beds also offers considerable potential for patient redistribution to minimize unmet hospital demand (Soroush et al. 2022). Finally, Guillon et al. (2021) examine large-scale patient transfers in France and find that inter-regional transfers of critically ill COVID-19 patients correlate with reduced mortality rates. A combination of modeling techniques and data-driven interventions can substantially enhance resource utilization, manage surges in demand, and improve patient outcomes during health crises such as COVID-19.

While reassigning patients can relieve stress on overcrowded hospitals, numerous studies caution that mobility itself can increase transmission if not carefully managed. Metapopulation network modeling reveals how transferring patients across regions can transform localized outbreaks into expansive epidemics (Calvetti et al. 2021). Real-world mobility data corroborate this, finding strong correlations between movement patterns and surges in infection rates (Badr et al. 2020). Some analyses dig deeper into specific transit corridors, illustrating that shared public transportation spaces can function as hot spots for repeated virus transmission (Mo et al. 2021). Large-scale mobility research likewise identifies inequalities in how certain communities bear disproportionate risks, prompting discussions on selective movement restrictions or additional targeted interventions (Chang, Pierson, et al. 2021; Chang, Wilson, et al. 2021). These insights reinforce that any patient-routing or resource-allocation strategy must account for how physical relocation might inadvertently spread disease, balancing short-term capacity relief against potential longer-term epidemiological consequences.

With this research in mind, there still remains a pressing need to integrate epidemiological insights with systematic patient and vaccine allocation strategies in pandemic scenarios, as patient movement can simultaneously address capacity constraints and exacerbate disease spread. To address these challenges, this study proposes a mixed-integer nonlinear programming model that integrates the Susceptible-Infected-Recovered-Vaccinated (SIRV) epidemic framework with a dynamic patient transfer and vaccine allocation framework. This model minimizes unmet demand for hospital

beds while accounting for the additional disease transmission caused by patient movements between regions. Unlike traditional models that often overlook the relationship between patient allocation and disease dynamics, this approach incorporates spatial and temporal constraints, healthcare capacities, and the effects of vaccination and immunity loss. Using real-world data from Florida's 67 counties during the COVID-19 pandemic, the model simulates patient allocation over multiple decision periods. By dynamically adjusting patient transfers and considering healthcare capacities, the model not only reduces unmet demand in populous metropolitan areas, but also minimizes unnecessary transfers, thereby alleviating the pressure on overburdened facilities.

## **2. Method**

### **2.1. SIRV Modeling**

The Susceptible-Infected-Recovered (SIR) epidemiological model of disease spread is a basic but popular method for predicting disease dynamics in a homogeneous population of individuals (Longini Jr 1986). The discretized difference equation formulation of the SIR model is

$$\begin{aligned} S^{t+1} &= S^t - \frac{\beta S^t I^t}{N} \\ I^{t+1} &= I^t + \frac{\beta S^t I^t}{N} - \gamma I^t \\ R^{t+1} &= R^t + \gamma I^t \end{aligned}$$

where  $S^t$ ,  $I^t$ ,  $R^t$  represent the number of susceptible, infected, and recovered individuals, respectively, at time  $t$ . The parameters  $\beta$  and  $\gamma$  denote the disease's transmission rate and recovery rate, respectively, and  $N$  represents the total population size.

The SIRV epidemiological model extends the basic SIR model to account for vaccination dynamics and immunity loss, making it suitable for predicting disease spread in a population with vaccination interventions. The discretized difference equation formulation of the SIRV model is given as:

$$\begin{aligned} S^{t+1} &= S^t - \frac{\beta S^t I^t}{N} - \lambda S^t + \omega V^t + q R^t \\ I^{t+1} &= I^t + \frac{\beta S^t I^t}{N} + \frac{\beta \ell V^t I^t}{N} - \gamma I^t \\ V^{t+1} &= V_i^t + \lambda S^t - \omega V^t - \frac{\beta \ell V^t I^t}{N} \\ R^{t+1} &= R^t + \gamma I^t - q R^t \end{aligned}$$

where  $S^t$ ,  $I^t$ ,  $R^t$ , and  $V^t$  represent the number of susceptible, infected, recovered, and vaccinated individuals, respectively, at time  $t$ . The parameters  $\beta$ ,  $\gamma$ ,  $\lambda$ ,  $q$ ,  $\omega$ , and  $\ell$  denote the disease's transmission rate, recovery rate, vaccination rate, natural immunity loss rate, vaccinated immunity loss rate, and leaky vaccine rate, respectively, while  $N$  represents the total population size.

### **2.2. Mathematical Model**

Given that the above SIRV model assumes a homogeneous mixing of the interacting population, we subdivide our population into  $n$  metapopulations. We incorporate the discretized and subdivided SIRV equations into our mathematical model as constraints to record the disease progression and behavior in terms of the number of susceptible, infected, recovered, and vaccinated individuals in each region across the time period and decision intervals. We also consider the effects of patient transfer and relocation when calculating the disease spread. Altogether, our mathematical model, which is an extension of the model found in Abazari et al. (2024), is formulated as:

$$\min \frac{1}{n} \sum_{i,t'} u_i^{t'} \quad (1)$$

subject to

$$S_i^{t+1} = S_i^t - \frac{\beta_i S_i^t I_i^t}{N_i} - \lambda_i S_i^t + \omega_i V_i^t + q_i R_i^t \quad \forall i, t \quad (2)$$

$$I_i^{t+1} = I_i^t + \frac{\beta_i S_i^t I_i^t}{N_i} + \frac{\beta_i \ell_i V_i^t I_i^t}{N_i} - \gamma_i I_i^t \quad \forall i, t \quad (3)$$

$$I_i^{t'+1} = I_i^{t'} + \frac{\beta_i S_i^{t'} I_i^{t'}}{N_i} + \frac{\beta_i \ell_i V_i^{t'} I_i^{t'}}{N_i} - \gamma_i I_i^{t'} + \sum_j (Z_{j,i}^{t'} - Z_{i,j}^{t'}) \quad \forall i, t' \quad (4)$$

$$V_i^{t+1} = V_i^t + \lambda_i S_i^t - \omega_i V_i^t - \frac{\beta_i \ell_i V_i^t I_i^t}{N_i} \quad \forall i, t \quad (5)$$

$$R_i^{t+1} = R_i^t + \gamma_i I_i^t - q_i R_i^t \quad \forall i, t \quad (6)$$

$$u_i^{t'} = \sum_{t \in \{t'-\psi+1, \dots, t'\}} \alpha_i^t I_i^t + \sum_{i \neq j} (Z_{j,i}^{t'} - Z_{i,j}^{t'}) - \phi_i^{t'} \quad \forall i, t' \quad (7)$$

$$\phi_i^{t'} \leq \gamma_i C_i \quad \forall i, t' \quad (8)$$

$$Z_{i,j}^{t'} \leq M \cdot A_{i,j}^{t'} \quad \forall i, t' \quad (9)$$

$$A_{i,j}^{t'} \cdot d_{ij} \leq D \quad \forall i, j, t' \quad (10)$$

$$Z_{i,j}^{t'} \geq A_{i,j}^{t'} \quad \forall i, j, t' \quad (11)$$

$$S_i^t, I_i^t, R_i^t, V_i^t \geq 0 \quad \forall i, t \quad (12)$$

$$u_i^{t'}, \phi_i^{t'} \geq 0 \quad \forall i, t' \quad (13)$$

$$Z_{i,j}^{t'} \geq 0 \quad \forall i, j, t' \quad (14)$$

The objective function (1) minimizes the average unmet hospital bed demand across counties. Constraint (2) models the evolution of the susceptible population, incorporating infection rates, vaccination rates, and immunity loss. Constraint (3) tracks the dynamics of the infected population, including new infections, recoveries, and vaccine leakages. Constraint (4) captures additional infection dynamics during decision periods, incorporating patient transfers. Constraint (5) models the vaccinated population's dynamics, accounting for vaccination rates, immunity loss, and vaccine inefficacy. Constraint (6) governs the recovered population's dynamics. Constraint (7) defines unmet demand based on infections, patient transfers, and satisfied demand. Constraint (8) ensures that satisfied demand does not exceed a county's healthcare capacity. Constraint (9) ensures that patient transfers between regions are limited to a large constant scaled by a binary indicator of whether the transfer occurs. Constraint (10) ensures that patient transfers between regions are allowed only if the distance between them does not exceed the maximum allowable threshold. Constraint (11) enforces that the number of patients transferred between regions is nonzero only if the corresponding binary transfer indicator is activated. Constraints (12)-(14) enforce non-negativity and consistency of decision variables. See Table 1 for description of the model sets, parameters, and decision variables.

### 2.2.1. Linearization

Due to the formulation of the SIRV epidemiological model, there arises nonlinearity in the constraints of our model. Specifically, constraints (2)-(4) have the number of susceptible and infected people multiplied together ( $S_i^t I_i^t$ ) and constraint (5) has the number of vaccinated and infected people multiplied together ( $V_i^t I_i^t$ ). It is often computationally expensive and inefficient to solve large-scale nonlinear models, thus we transform our nonlinear constraints via McCormick Envelopes to linearize them (McCormick 1976). Linearization ensures that the mathematical model is easier to solve computationally while retaining the model's accuracy.

McCormick Envelopes are used to linearize bivariable nonlinear equations where each variable has specific upper and lower bounds. Given an equation  $z = xy$ , where  $x$  and  $y$  are variables with upper and lower bounds  $x_u, y_u$  and  $x_l, y_l$ ,

**Table 1.** Model Component Notation

Category	Symbol	Description
<b>Sets</b>	$i$	Set of regions (counties), $i \in \{1, \dots, n\}$ .
	$j$	Set of regions (counties), $j \in \{1, \dots, n\}$ .
	$t$	Set of time periods, $t = \{t_0, t_0 + 1, \dots, t_f\}$ .
	$t'$	Set of decision-making time periods, $t' = \{t_0, t_0 + \psi, \dots, t_f\}$ .
<b>Parameters</b>	$S_i^0, I_i^0, R_i^0, V_i^0$	Initial susceptible, infected, recovered, and vaccinated individuals in county $i$ .
	$N_i$	Population of county $i$ .
	$\beta_i$	Infection rate of county $i$ .
	$\gamma_i$	Recovery rate of county $i$ .
	$\lambda_i$	Vaccination rate of county $i$ .
	$q_i$	Loss of natural immunity rate of county $i$ .
	$\omega_i$	Loss of vaccinated immunity rate of county $i$ .
	$\ell_i$	Leaky vaccine rate of county $i$ .
	$\alpha_i^{t'}$	Hospital beds per infection of county $i$ at decision period $t'$ .
	$d_{ij}$	Distance between counties $i$ and $j$ .
	$C_i$	Healthcare capacity of county $i$ .
	$n$	Number of counties.
	$D$	Maximum allowable distance for patient allocation.
	$M$	A large number.
	$\psi$	Decision-making time intervals (e.g. 7, 14, or 21 days).
	$t_0, t_f$	Beginning and ending time of study period.
<b>Decision Variables</b>	$S_i^t, I_i^t, R_i^t, V_i^t$	Susceptible, infected, recovered, and vaccinated individuals in county $i$ in period $t$ .
	$u_i^{t'}$	Number of unmet demand in county $i$ at decision period $t'$ .
	$Z_{ij}^{t'}$	Number of patients moved from county $i$ to $j$ at decision period $t'$ .
	$\phi_i^{t'}$	Satisfied demand in county $i$ at decision period $t'$ .
	$A_{ij}^{t'}$	1, if patients are transferred from county $i$ to $j$ at decision period $t'$ , 0 otherwise.

respectively, the general linearization becomes

$$\begin{aligned}
 \min \quad & z \\
 \text{s.t.} \quad & z \geq x_l y + x y_l - x_l y_l \\
 & z \geq x_u y + x y_u - x_u y_u \\
 & z \leq x_u y + x y_l - x_u y_l \\
 & z \leq x y_u + x_l y - x_l y_u.
 \end{aligned}$$

In our model, we transform our nonlinear constraints (2)-(5) as follows. We set the upper and lower bounds of  $S_i^t I_i^t, V_i^t$  as 0 and  $N_i$ , respectively, and make the substitutions  $Y_i^t = S_i^t I_i^t$  and  $W_i^t = V_i^t I_i^t$ . Thus our linearized constraints

(2')-(5') become

$$S_i^{t+1} = S_i^t - \frac{\beta_i Y_i^t}{N_i} - \lambda_i S_i^t + \omega_i V_i^t + q_i R_i^t \quad \forall i, t \quad (2')$$

$$I_i^{t+1} = I_i^t + \frac{\beta_i Y_i^t}{N_i} + \frac{\beta_i \ell_i W_i^t}{N_i} - \gamma_i I_i^t \quad \forall i, t \quad (3')$$

$$I_i^{t'+1} = I_i^{t'} + \frac{\beta_i Y_i^{t'}}{N_i} + \frac{\beta_i \ell_i W_i^{t'}}{N_i} - \gamma_i I_i^{t'} + \sum_j (Z_{j,i}^{t'} - Z_{i,j}^{t'}) \quad \forall i, t' \quad (4')$$

$$V_i^{t+1} = V_i^t + \lambda_i S_i^t - \omega_i V_i^t - \frac{\beta_i \ell_i W_i^t}{N_i} \quad \forall i, t \quad (5')$$

and we add the following constraints:

$$Y_i^t \geq 0 \quad \forall i, t \quad (15)$$

$$Y_i^t \geq N_i S_i^t + N_i I_i^t - N_i^2 \quad \forall i, t \quad (16)$$

$$Y_i^t \leq N_i S_i^t \quad \forall i, t \quad (17)$$

$$Y_i^t \leq N_i I_i^t \quad \forall i, t \quad (18)$$

$$W_i^t \geq 0 \quad \forall i, t \quad (19)$$

$$W_i^t \geq N_i V_i^t + N_i I_i^t - N_i^2 \quad \forall i, t \quad (20)$$

$$W_i^t \leq N_i V_i^t \quad \forall i, t \quad (21)$$

$$W_i^t \leq N_i I_i^t \quad \forall i, t \quad (22)$$

### 2.2.2. Model Assumptions

As our model is an extension of that found in Abazari et al. (2024), we employ many of the same assumptions: (1) The total capacity of healthcare facilities is constant and does not change over time; (2) Patients may be transferred to other regions, provided the distance is within a predefined reasonable limit; (3) The decision-making horizon is ten days; (4) All patients within a region are assumed to have the same recovery time; (5) Regions are permitted to both send and receive patients from other regions during the given time frame; (6) The healthcare facilities within each region are aggregated into a single value, representing the total capacity for that region; (7) Distances between regions are calculated based on roadway travel distances; (8) Assigning patients to different regions does not influence the number of beds required per infection.

With the inclusion of our vaccination dynamics, we include the following new assumptions: (9) Vaccines are administered at a constant rate which is applied uniformly across the susceptible metapopulations; (10) If an individual receives a vaccine, then they receive immediate immunity, i.e., there is no delay in the increase in vaccine efficacy; (11) A vaccinated individual's immunity wanes at a constant rate; (12) All administered vaccines are leaky, i.e., vaccine-induced protection lowers, but does not eliminate susceptibility or infection risk; (13) There is no difference in recovery rates or healthcare between vaccinated and unvaccinated individuals; (14) There are no side effects or mortality due to vaccination; (15) Individuals only receive one vaccination, i.e., there are no boosters administered; (16) There is uniform access and acceptance of vaccination between all metapopulations.

### 2.2.3. Study Area and Parameter Estimation

The number of hospital beds required per infection,  $\alpha_i^t$ , for county  $i$  at time  $t$ , was derived using time series data (Abazari et al. 2024). This calculation is crucial for assessing unmet hospital demand in Florida counties. Initially, the daily hospitalized patient count  $H_i^t$  was calculated using data from NIEHS (2023) by multiplying the percentage of utilized hospital beds (PctBeds) by the number of available staffed beds (Staffed.All.Beds). Daily confirmed COVID-19 cases,  $I_i^t$ , from USF (2023) were used to compute  $\alpha_i^t$  using the equation:

$$\alpha_i^t = \frac{H_i^t}{I_i^t}.$$

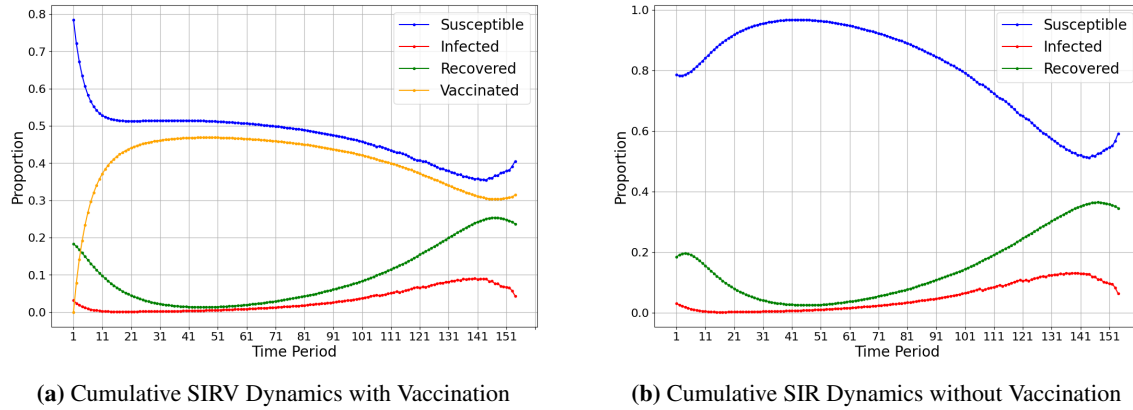


**Figure 1.** Comparison of Cumulative SIRV and SIR Dynamics in Florida

This value represents the upper limit of the 95% confidence interval from the hierarchical time series models used in the analysis.

The authors in Abazari et al. (2024) also utilized the SIR modeling framework to estimate the infection and recovery rates ( $\beta_i$  and  $\gamma_i$ ) on a per-county basis, and to calculate the initial number of susceptible, infected, and recovered individuals ( $S_i^0, I_i^0, R_i^0$ ) for the case study. To derive these parameters, the first forty days of the study period were analyzed using a robust maximum likelihood estimation method. The infection and recovery rates were also assumed to remain constant throughout the mathematical model's progression.

For the vaccine parameters related to effectiveness, we harnessed data from Zheng et al. (2022) and set  $\omega_i = 0.109$  and  $\ell_i = 0.3$  for each county. The remaining parameters were selected using an empirical approach, thus we set  $q_i = 0.08$  and  $\lambda_i = 0.1$  for each county. Finally, the maximum allowable travel distance was set to  $D = 70\text{mi}$ .

### 3. Results

In this section, we present the results of the mathematical model solved using the Florida case study in a vaccinated and unvaccinated scenario. The model was solved using the CPLEX solver on GAMS software using all the aforementioned parameters.

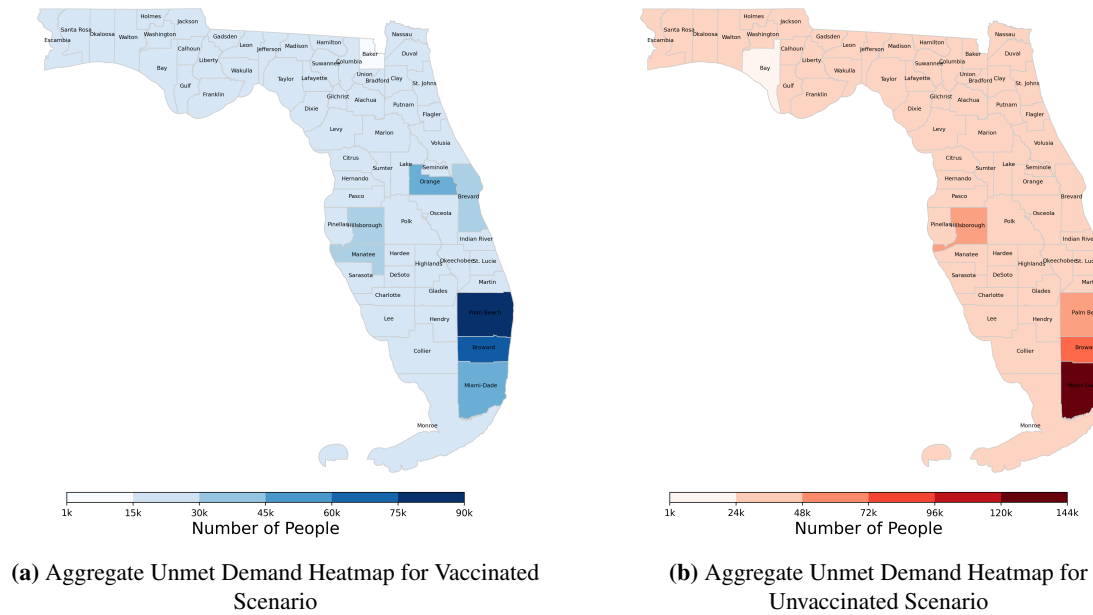
#### 3.1. SIRV Dynamics

Figure 1a demonstrates the proportions of the SIRV compartments of our model over the time horizon, with a notable late-stage increase in susceptibility and infections. This rise is driven by waning immunity, where previously recovered individuals lose natural immunity, thus reentering the susceptible group, and vaccinated individuals experience immunity loss, reducing the vaccinated population. As immunity declines and the vaccinated (and thus protected) population decreases, a “second-wave” of infection emerges, leading to a resurgence of the susceptible and infected populations. This phenomenon highlights the need for booster vaccines to prevent late stage or other immunity-retaining strategies to late resurgences of disease spread.

When comparing the SIRV dynamics between vaccinated and unvaccinated scenarios, Figure 1b reveals how the number of susceptible individuals is significantly lower in the vaccinated case, consistent with the expected impact of vaccination. There is also a significant drop in the number of susceptible individuals in the vaccinated scenario due to the impact of vaccines whereas in the unvaccinated scenario, there is a more gradual decline as susceptible individuals become infected. The infected population in the unvaccinated scenario also peaks higher than in the vaccinated scenario, indicating the higher transmission risk associated with a lack of disease prevention and intervention. Finally, the recovered population in the unvaccinated scenario peaks higher than in the vaccinated scenario because vaccinated individuals are less likely to become infected, reducing the overall number of individuals who recover from the disease.

#### 3.2. Unmet Demand

Figure 2 displays the aggregate unmet demand that each Florida county attains during the time horizon. We observe in Figure 2a that in the vaccinated scenario, the vast majority of unmet hospital demand aggregates in south Florida's populous counties like Palm Beach, Broward, and Miami-Dade with Palm Beach approaching an unsatisfied population of ninety thousand. Central Florida also experiences a considerable amount of unmet demand, especially in



**Figure 2.** Comparison of Aggregate Unmet Demand in Vaccinated vs. Unvaccinated Scenarios

Orange, Brevard, Hillsborough, and Monroe counties, though at a lower level. Moving north through Florida to the more rural counties, there is little unmet hospital demand compared to its southern counterparts, with Baker county achieving the smallest unmet demand throughout the case study.

In the unvaccinated scenario, depicted in Figure 2b, the large south Florida metropolitan areas experience considerably more unmet demand. Miami-Dade county experiences nearly 144 thousand unsatisfied individuals, followed by Broward and Palm Beach counties with over fifty and seventy-five thousand unsatisfied individuals, respectively. Central Florida attains only minimally more unmet demand, highlighted by Hillsborough county, and the more rural counties in the Panhandle, especially Bay county, attain comparatively distributed and low levels of unmet hospital demand.

The spatial distribution of unmet hospital demand demonstrates where vital healthcare resources and preventative measures, like vaccines, are critical to minimize disease spread, and thus unmet hospital demand and strain on the healthcare system. Large metropolitan areas may require increased resource allocation and strategic planning to prevent hospital overcrowding and ensure adequate care for their larger infected populations. In contrast, rural areas, which experience lower patient transfer volumes and fewer total infections, generally face less strain on their healthcare systems and can manage demand more effectively.

### 3.3. Patient Transfers

Patient transfers play a critical role in the transmission of infectious diseases, thus they were tracked on all decision periods of our mathematical model. Figure 3 displays the patient transfer information for Days 30 and 90 of the model. The thickness of the arrow dictates the volume of the patient transfer, and the direction of the arrow, from tail to tip, demonstrates patients being transferred from county  $i$  to county  $j$ .

We omit the graphs of the daily in- and out-degrees of each county for Florida patient travel in both scenarios, though we list some of the key insights they reveal. In the vaccinated scenario, as outlined in Figure 3a large metropolitan counties like Palm Beach, Orange, and Duval counties repeatedly appear as “receivers” of large patient volumes. In general, the large metropolitan areas often send and receive large volumes of patients as they have larger hospital capacities, though a larger number of infections. Other more rural counties, like those in the Panhandle, regularly export patients to nearby regions since they tend to have limited healthcare capacity relative to their infection surges, making them consistent “senders”. We also observe that with the waning of vaccine effectiveness and immunity observed in Figure 1a, patient transfer drastically increases to account for the surge in infections. Finally, patient transfers occurred consistently throughout the time horizon, indicating that despite vaccination efforts, hospital capacity constraints re-



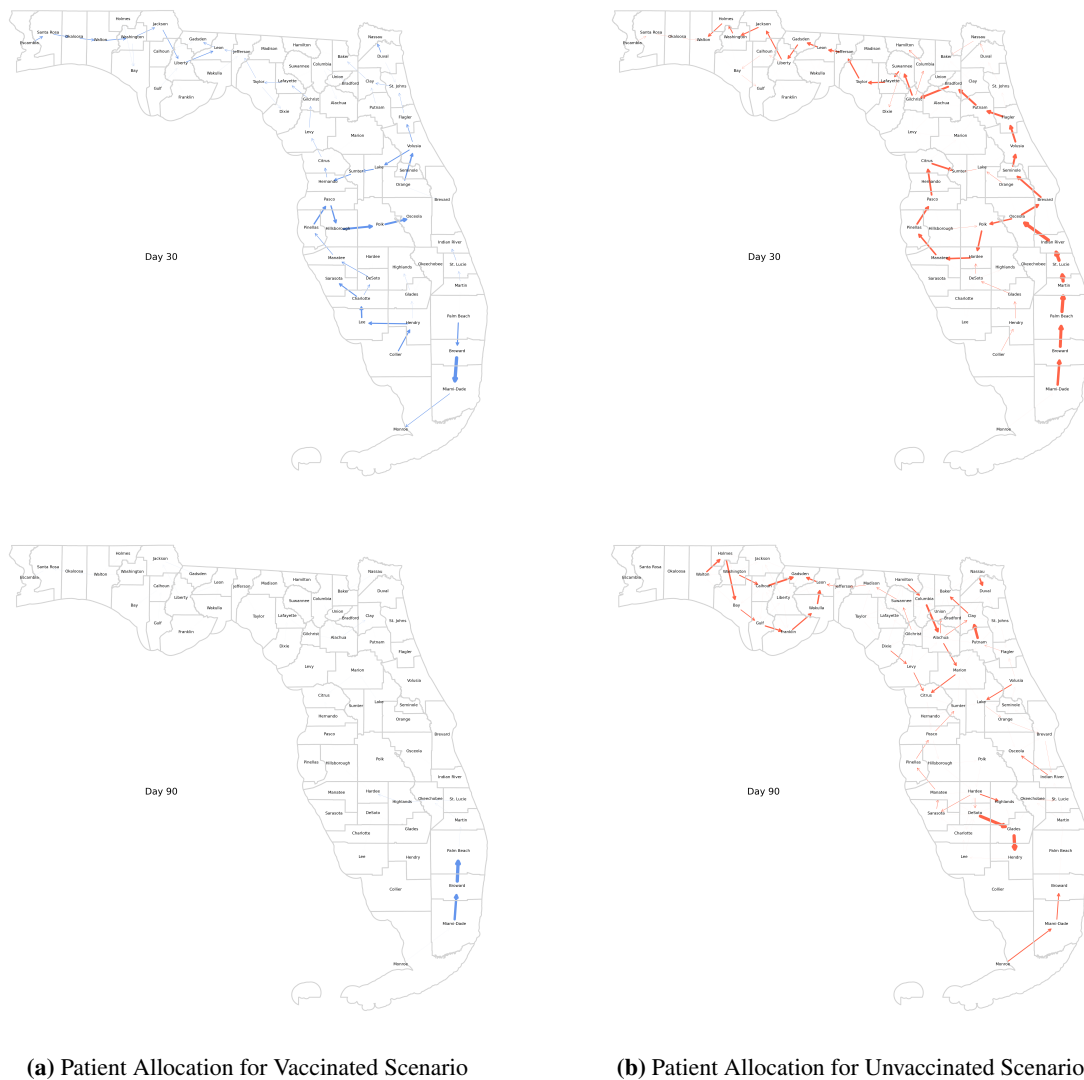


**Figure 3.** Comparison of Patient Allocation in Vaccinated vs. Unvaccinated Scenarios

mained a persistent challenge, necessitating ongoing redistribution of patients to balance demand across regions.

Figure 3b portrays how in the unvaccinated scenario, due to a higher peak of infection levels than in the vaccinated scenario, overall patient transfers tend to be larger and occur more frequently. The receivers once again included metropolitan areas with large hospital capacities, including Miami-Dade, Broward, Hillsborough, Orange, and Duval counties, and the senders included rural counties in the Panhandle that did not possess the hospital resources to handle surges in infection and hospital demand. Unlike in the vaccinated scenario, patient transfers were initially very high, later decreasing, before finally increasing once again during the “second wave” of infections.

We also note a common phenomenon that results from constraints (9)-(11), that is, the “chaining” of patients being transferred to subsequent adjacent counties. Patient transfers create cascading effects during decision periods as hospitals reach capacity. When transferred patients fill available beds in receiving counties, remaining patients requiring care must be redirected elsewhere, leading to further transfers. In general, we observe less transferred patients for the vaccinated scenario (953 thousand) than the unvaccinated scenario (1.10 million).

#### 4. Conclusions and Future Work

This research presents a data-driven mixed-integer nonlinear programming model that integrates SIRV epidemic dynamics with patient transfer decisions to minimize unmet hospital demand during pandemics. By leveraging real-world COVID-19 and Florida healthcare data, the model demonstrates how vaccination and interregional patient transfers interact to affect overall health outcomes. We observe how larger metropolitan regions frequently receive an influx of transferred patients, whereas rural areas often transfer patients away, thus underscoring the importance of geographically targeted strategies. Incorporating vaccines into the framework helped minimize peak infections, though we note how waning vaccination and natural immunity leads to secondary infection surges and heightened patient transfers. Coordinated vaccination efforts and patient transfer strategies are pivotal for alleviating stress on burdened healthcare facilities to better balance healthcare capacity.

Despite these contributions, the authors highlight several of the aforementioned model assumptions that must be addressed. The vaccine-related parameters were assumed to be the same for all metapopulations and be constant throughout the time horizon. Patient “chaining” was also a significant issue wherein individuals were re-transferred across multiple counties as they each reached their healthcare capacity. The mathematical model also did not account for demographic or socioeconomic heterogeneity, which could influence disease spread and vaccine effectiveness.

Recognizing limitations like these provides direction on how to strengthen the applicability and realism of the model, thus we propose the following examples. Future research can enhance this model by incorporating demographic and socioeconomic factors such as age, underlying health conditions, and income levels to highlight disparities in disease burden and vaccine access, enabling more equitable resource allocation. Explicitly modeling vaccine distribution, including the number of doses supplied to each region and its logistical challenges, would improve the model’s relevance to real-world vaccination efforts. Allowing parameters such as infection, recovery, and vaccination rates to vary over time could better reflect dynamic factors like emerging variants, seasonal trends, and shifting public health policies. Refining patient transfer constraints by limiting re-transfers or imposing higher penalties for multiple hand-offs would reduce unrealistic “chaining” effects and provide a more accurate depiction of patient flows. Additionally, calibrating vaccination parameters with time-series data would capture the effects of booster campaigns and vaccine waning more precisely. Finally, introducing stochastic elements to represent random variations in infection spread and hospital arrivals would create a more realistic model, enabling policymakers to evaluate strategies under varying levels of uncertainty.

#### References

- Abazari, S., Alisan, O., Vanli, O. A., and Ozguven, E. E. (May 2024). “Data-Driven Patient Allocation for Healthcare Facility Optimization Under Uncertainty with SIR Dynamics”. *2024 IIE Annual Conference and Expo*. IIE.
- Anastassopoulou, C., Russo, L., Tsakris, A., and Siettos, C. (2020). “Data-based analysis, modelling and forecasting of the COVID-19 outbreak”. *PLoS one* 15.3, e0230405.
- Aydin, N. and Cetinkale, Z. (2022). “Analyses on ICU and non-ICU capacity of government hospitals during the COVID-19 outbreak via multi-objective linear programming: An evidence from Istanbul”. *Computers in Biology and Medicine* 146, p. 105562.
- Badr, H. S., Du, H., Marshall, M., Dong, E., Squire, M. M., and Gardner, L. M. (2020). “Association between mobility patterns and COVID-19 transmission in the USA: a mathematical modelling study”. *The Lancet Infectious Diseases* 20.11, pp. 1247–1254.
- Bennouna, A., Joseph, J., Nze-Ndong, D., Perakis, G., Singhvi, D., Lami, O. S., Spantidakis, Y., Thayaparan, L., and Tsiourvas, A. (2023). “COVID-19: Prediction, prevalence, and the operations of vaccine allocation”. *Manufacturing & Service Operations Management* 25.3, pp. 1013–1032.
- Calvetti, D., Hoover, A., Rose, J., and Somersalo, E. (2021). *Modeling Epidemic Spread among a Commuting Population Using Transport Schemes*. *Mathematics* 2021, 9, 1861.
- Chang, S., Pierson, E., Koh, P. W., Gerardin, J., Redbird, B., Grusky, D., and Leskovec, J. (2021). “Mobility network models of COVID-19 explain inequities and inform reopening”. *Nature* 589.7840, pp. 82–87.
- Chang, S., Wilson, M. L., Lewis, B., Mehrab, Z., Dudakiya, K. K., Pierson, E., Koh, P. W., Gerardin, J., Redbird, B., Grusky, D., et al. (2021). “Supporting covid-19 policy response with large-scale mobility-based modeling”. *Proceedings of the 27th ACM SIGKDD Conference on Knowledge Discovery & Data Mining*, pp. 2632–2642.
- Crokidakis, N. (2020). “Modeling the early evolution of the COVID-19 in Brazil: Results from a Susceptible–Infectious–Quarantined–Recovered (SIQR) model”. *International Journal of Modern Physics C* 31.10, p. 2050135.

- Della Rossa, F., Salzano, D., Di Meglio, A., De Lellis, F., Coraggio, M., Calabrese, C., Guarino, A., Cardona-Rivera, R., De Lellis, P., Liuzza, D., et al. (2020). "A network model of Italy shows that intermittent regional strategies can alleviate the COVID-19 epidemic". *Nature communications* 11.1, p. 5106.
- Dijkstra, S., Baas, S., Braaksma, A., and Boucherie, R. J. (2023). "Dynamic fair balancing of COVID-19 patients over hospitals based on forecasts of bed occupancy". *Omega* 116, p. 102801.
- Eriskin, L., Karatas, M., and Zheng, Y.-J. (2024). "A robust multi-objective model for healthcare resource management and location planning during pandemics". *Annals of Operations Research* 335.3, pp. 1471–1518.
- Guillon, A., Laurent, E., Godillon, L., Kimmoun, A., and Grammatico-Guillon, L. (2021). "Inter-regional transfers for pandemic surges were associated with reduced mortality rates". *Intensive Care Medicine* 47.7, pp. 798–800.
- He, S., Peng, Y., and Sun, K. (2020). "SEIR modeling of the COVID-19 and its dynamics". *Nonlinear dynamics* 101, pp. 1667–1680.
- Hong, Z., Li, Y., Gong, Y., and Chen, W. (2024). "A data-driven spatially-specific vaccine allocation framework for COVID-19". *Annals of Operations Research* 339.1, pp. 203–226.
- Hou, C., Chen, J., Zhou, Y., Hua, L., Yuan, J., He, S., Guo, Y., Zhang, S., Jia, Q., Zhao, C., et al. (2020). "The effectiveness of quarantine of Wuhan city against the Corona Virus Disease 2019 (COVID-19): A well-mixed SEIR model analysis". *Journal of medical virology* 92.7, pp. 841–848.
- Hu, J., Hu, G., Cai, J., Xu, L., and Wang, Q. (2020). "Hospital bed allocation strategy based on queuing theory during the covid-19 epidemic". *Cmc-Comput. Mater. Contin.* 66, pp. 793–803.
- Klein, M. G., Cheng, C. J., Lii, E., Mao, K., Mesbahi, H., Zhu, T., Muckstadt, J. A., and Hupert, N. (2022). "COVID-19 models for hospital surge capacity planning: a systematic review". *Disaster medicine and public health preparedness* 16.1, pp. 390–397.
- Kozioł, K., Stanisławski, R., and Bialic, G. (2020). "Fractional-order sir epidemic model for transmission prediction of covid-19 disease". *Applied Sciences* 10.23, p. 8316.
- Lauer, S. A., Grantz, K. H., Bi, Q., Jones, F. K., Zheng, Q., Meredith, H. R., Azman, A. S., Reich, N. G., and Lessler, J. (2020). "The incubation period of coronavirus disease 2019 (COVID-19) from publicly reported confirmed cases: estimation and application". *Annals of internal medicine* 172.9, pp. 577–582.
- Li, Q., Tang, B., Bragazzi, N. L., Xiao, Y., and Wu, J. (2020). "Modeling the impact of mass influenza vaccination and public health interventions on COVID-19 epidemics with limited detection capability". *Mathematical biosciences* 325, p. 108378.
- Longini Jr, I. M. (1986). "The generalized discrete-time epidemic model with immunity: a synthesis". *Mathematical biosciences* 82.1, pp. 19–41.
- Ma, X., Zhao, X., and Guo, P. (2022). "Cope with the COVID-19 pandemic: Dynamic bed allocation and patient subsidization in a public healthcare system". *International Journal of Production Economics* 243, p. 108320.
- McCormick, G. P. (1976). "Computability of global solutions to factorable nonconvex programs: Part I—Convex underestimating problems". *Mathematical programming* 10.1, pp. 147–175.
- Meyerowitz-Katz, G. and Merone, L. (2020). "A systematic review and meta-analysis of published research data on COVID-19 infection fatality rates". *International Journal of Infectious Diseases* 101, pp. 138–148.
- Mo, B., Feng, K., Shen, Y., Tam, C., Li, D., Yin, Y., and Zhao, J. (2021). "Modeling epidemic spreading through public transit using time-varying encounter network". *Transportation Research Part C: Emerging Technologies* 122, p. 102893.
- NIEHS (2023). *COVID-19 PVI Data*. <https://github.com/COVID19PVI/data/>. Accessed: March 2023.
- Parker, F., Sawczuk, H., Ganjkanloo, F., Ahmadi, F., and Ghobadi, K. (2020). "Optimal resource and demand redistribution for healthcare systems under stress from COVID-19". *arXiv preprint arXiv:2011.03528*.
- Queiroz, M. M., Ivanov, D., Dolgui, A., and Fosso Wamba, S. (2022). "Impacts of epidemic outbreaks on supply chains: mapping a research agenda amid the COVID-19 pandemic through a structured literature review". *Annals of operations research* 319.1, pp. 1159–1196.
- Sarkar, S., Pramanik, A., Maiti, J., and Reniers, G. (2021). "COVID-19 outbreak: A data-driven optimization model for allocation of patients". *Computers & Industrial Engineering* 161, p. 107675.
- Shi, F. (2023). "A Data-Driven Optimization Model for Medical Resource Allocation during the Pandemic". PhD thesis. Concordia University.
- Soroush, F., Nabilou, B., Faramarzi, A., and Yusefzadeh, H. (2022). "A study of the evacuation and allocation of hospital beds during the Covid-19 epidemic: a case study in Iran". *BMC Health Services Research* 22.1, p. 864.
- USF (2023). *Florida COVID-19 Hub*. <https://covid19-usflibrary.hub.arcgis.com/>. Accessed: March 2023.

- Waseel, F., Streftaris, G., Rudrusamy, B., and Dass, S. C. (2024). “Assessing the dynamics and impact of COVID-19 vaccination on disease spread: A data-driven approach”. *Infectious Disease Modelling* 9.2, pp. 527–556.
- Yinusa, A. and Faezipour, M. (2023). “Optimizing healthcare delivery: a model for staffing, patient assignment, and resource allocation”. *Applied System Innovation* 6.5, p. 78.
- Zheng, C., Shao, W., Chen, X., Zhang, B., Wang, G., and Zhang, W. (2022). “Real-world effectiveness of COVID-19 vaccines: a literature review and meta-analysis”. *International journal of infectious diseases* 114, pp. 252–260.

## **Biographies**

**Alexander DeLise** is a second-year undergraduate student at Florida State University in pursuit of a B.S. in Applied and Computational Mathematics and B.S. in Computational Science. His research interests include the field of Operations Research, Industrial Engineering, Optimization, and Quantum Information Science.

**Seyedreza Abazari** is a....

**Dr. Arda Vanli** is a Professor in the Industrial and Manufacturing Engineering (IME) Department at Florida A&M University and Florida State University, College of Engineering. Dr. Vanli’s research interests lie in the general area of applied industrial statistics and data analytics with applications in quality and reliability improvement in modern manufacturing processes, risk and vulnerability analysis for natural disasters and infectious disease data analysis. His research is published in journals including, Quality Engineering, Quality and Reliability Engineering International, Technometrics, IIE Transactions, IEEE Transactions on Semiconductor Manufacturing and Mechanical Systems and Signal Processing. He completed his Ph.D. in Industrial Engineering and Operations Research at the Pennsylvania State University, University Park, in August 2007. He received his M.S. degree in Mechanical Engineering from the Pennsylvania State University, University Park, PA in 2000 and his B.S. degree in Mechanical Engineering from the Middle East Technical University, Ankara, Turkey in 1998.